Acid−Base Catalysis in the Extradiol Catechol Dioxygenase Reaction Mechanism: Site-Directed Mutagenesis of His-115 and His-179 in *Escherichia coli* 2,3-Dihydroxyphenylpropionate 1,2-Dioxygenase (MhpB)[†,‡]

Sharon Mendel, Andrew Arndt, and Timothy D. H. Bugg*

Department of Chemistry, University of Warwick, Coventry CV4 7AL, U.K.

Received July 13, 2004; Revised Manuscript Received August 20, 2004

ABSTRACT: The extradiol catechol dioxygenases catalyze the non-heme iron(II)-dependent oxidative cleavage of catechols to 2-hydroxymuconaldehyde products. Previous studies of a biomimetic model reaction for extradiol cleavage have highlighted the importance of acid−base catalysis for this reaction. Two conserved histidine residues were identified in the active site of the class III extradiol dioxygenases, positioned within 4−5 Å of the iron(II) cofactor. His-115 and His-179 in *Escherichia coli* 2,3-dihydroxyphenylpropionate 1,2-dioxygenase (MhpB) were replaced by glutamine, alanine, and tyrosine. Each mutant enzyme was catalytically inactive for extradiol cleavage, indicating the essential nature of these acid−base residues. Replacement of neighboring residues Asp-114 and Pro-181 gave D114N, P181A, and P181H mutant enzymes with reduced catalytic activity and altered pH/rate profiles, indicating the role of His-179 as a base and His-115 as an acid. Mutant H179Q was catalytically active for the lactone hydrolysis half-reaction, whereas mutant H115Q was inactive, implying a role for His-115 in lactone hydrolysis. A catalytic mechanism involving His-179 and His-115 as acid−base catalytic residues is proposed.

The non-heme iron(II)-dependent catechol dioxygenases catalyze the oxidative cleavage of catechol substrates to give 2-hydroxy-6-keto-hexa-2,4-dienoic acid products (see Figure 1) as part of bacterial catabolic pathways used for the degradation of aromatic compounds in the soil (*1*, *2*). Three classes of extradiol catechol dioxygenases are found, each of which require iron(II) for activity (*3*): class 1 enzymes are monomeric 20−25 kDa enzymes; class 2 enzymes are tetrameric enzymes of subunit 35 kDa, typefied by 2,3-dihydroxybiphenyl 1,2-dioxygenase (BphC); class 3 enzymes also contain a catalytic 35 kDa subunit, which in the case of *Escherichia coli* MhpB[1] is an α_4 tetramer while in the case of protocatechuate 4,5-dioxygenase (LigAB) is an $\alpha_2\beta_2$ tetramer. X-ray crystal structures of both BphC (*4*) and LigAB (*5*) have been solved: in each case, the active site contains a mononuclear iron(II) center ligated by two histidine and one glutamic acid ligands (see Figure 2).

Mechanistic studies on 2,3-dihydroxyphenylpropionate 1,2-dioxygenase from *Escherichia coli* (of class III) have established the intermediacy of a seven-membered lactone intermediate (*6*), formed by Criegee rearrangement of a proximal hydroperoxide intermediate substituted at C-2 (*7*), as shown in Figure 1. Studies of a biomimetic model reaction for extradiol cleavage, involving iron(II) chloride/1,4,7-triazacyclononane/pyridine/methanol, have revealed a requirement for a base, which generates the catecholate monoanion, and a proton donor, for acid catalysis of the Criegee rearrangement (*8*, *9*).

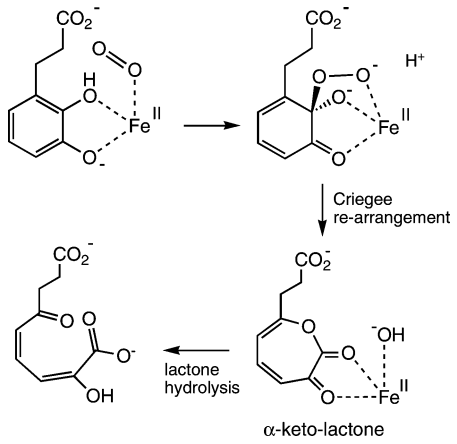

FIGURE 1: Extradiol cleavage reaction catalyzed by 2,3-dihydroxyphenylpropionate 1,2-dioxygenase (MhpB) showing the proximal hydroperoxide and α-keto lactone reaction intermediates.

In the X-ray crystal structure of protocatechuate 4,5-dioxygenase from *Sphingomonas* (*5*), there are two additional acid−base residues within 4 Å of the iron(II) center, His-195 and His-127 (see Figure 2A). Sequence alignment of class III extradiol dioxygenases (see Figure 2B) reveals that His-195 is completely conserved (found as His-179 in *E. coli* MhpB). His-127 is conserved in all but two sequences, those of *Pseudomonas pseudoalcaligenes* 2-aminophenol 1,6-dioxygenase (*10*) and human 3-hydroxyanthranilate dioxygenase (*11*), in which His-127 (found as His-115 in *E. coli* MhpB) is replaced by tyrosine. Adjacent to His-127 is a

[†] This work was funded by BBSRC (Research Grant B16501), and a grant (to A.A.) from Wake Forest University.

[‡] This paper is dedicated to Prof. Chris Walsh (Harvard Medical School) on the occasion of his 60th birthday.

* Tel 44-2476-573018; fax 44-2476-524112; E-mail T.D.Bugg@warwick.ac.uk.

[1] Abbreviations: EDTA, ethylene 1,2-diamine tetracetic acid; HPLC, high-performance liquid chromatography; MBP, maltose binding protein; MhpB, 2,3-dihydroxyphenylpropionate 1,2-dioxygenase.

10.1021/bi048518t CCC: $27.50
Published on Web 10/02/2004

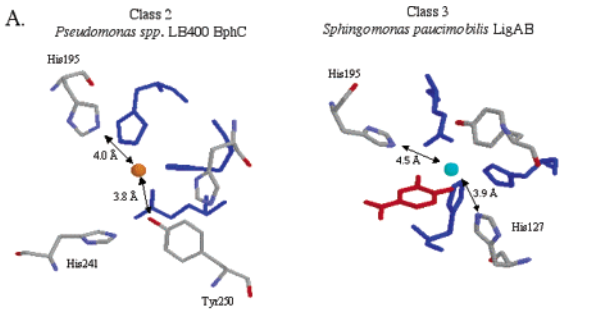

B.

	115	179	% identity
E. coli MhpB	SYCMQV**DH**GFAQPL	GSGGLS**HQP**PVPE	100
P. putida MhpB	SYRMQV**DH**GFAQPL	GSGGLS**HQP**PVPE	70
A.eutrophus MpcI	SHRMQV**DH**GCADAL	GSGGIS**HEP**PVPE	54
Rhodococcus HppB	SRQMEV**DH**GAVQPM	GSGGLS**HDP**PVPQ	48
C. testosteroni	SRRMLV**DH**GFSQAL	GSGGLS**HEP**PVPT	44
4,5-PCD LigB	MNQMDV**DH**GCTVPL	GTGGMS**HQL**QGPR	30
Burkholderia	SKSLVL**DH**SATVPI	GTGGLS**HWP**GMAE	25
Sphingomonas	INEMDV**DH**GLTVPM	GTGGMS**HQL**QGPR	24
P. pseud. AmnB	NPRFRV**DY**DTITTL	ASNTLS**HWH**FNQE	26
Human HAO	VLFEKW**FY**CKDLGT	DAWLDS**HHR**ELQA	20

FIGURE 2: Position of proposed acid−base residues in extradiol dioxygenase active sites: (A) active site structures for class II (*Pseudomonas sp*. LB400 BphC) and class III (*Sphingomonas paucimobilis* LigAB) extradiol dioxygenases, illustrating the positions of putative acid−base residues, prepared using Rasmol; (B) alignment of amino acid sequences of class III extradiol dioxygenases in proximity to His-115 and His-179 (with % amino acid sequence identity to MhpB sequence). Sequences are from the following organisms: *Escherichia coli* K12 (MhpB), *Pseudomonas putida* (MhpB), *Alcaligenes eutrophus* (MpcI), *Rhodococcus globerulus* PWD1 (HppB; *23*), *Comamonas testosteroni* TA441 (MhpB; *24*), *Burkholderia sp.* RP007 (PhnC; *25*), *Sphingomonas* (MhpB), *Sphingomonas paucimobilis* protocatechuate 4,5-dioxygenase (LigB), *Pseudomonas pseudoalcaligenes* JS45 2-aminophenol 1,6 dioxygenase (AmnB; *10*), and human 3-hydroxyanthranilate dioxygenase (HAO; *11*). The positions occupied by Asp-114, His-115, His-179, and Pro-181 (in MhpB sequence) are shown in bold.

conserved aspartic acid (Asp-126, found as Asp-114 in MhpB), whose side chain is positioned within 4−5 Å of the imidazole side chain of His-127 (see Figure 2A). To examine the role of His-179 and His-115 in extradiol dioxygenase catalysis, we have replaced His-179 and His-115 in MhpB by glutamine, alanine, and tyrosine, using site-directed mutagenesis. Here we report the activity of a series of mutant enzymes and an analysis of the effects of amino acid replacements.

MATERIALS AND METHODS

Materials. 2,3-Dihydroxyphenylpropionic acid was prepared using a published procedure (*12*). Restriction enzymes and T4 DNA ligase were obtained from New England BioLabs. Yeast extract, peptone, and agar were from Duchefa Biochemie. All other materials were of analytical grade.

Construction of MBP−MhpB Wild-Type and Mutated Fusion MhpB. The cloned gene (*mhpB*) was inserted into the pMAL-2 vector, downstream from the *malE* gene of *E. coli* under the control of the *tac* promoter, resulting in the expression of an maltose-binding protein (MBP) fusion protein. Restriction enzymes *Eco*RI and *Xba*I were used for the MBP−MhpB fusion (according to NEB Inc. Protein fusion & purification (pMAL) system manual). Plasmids encoding each of the mutated MBP−MhpBs were created by the method of splicing by overlap extension (*13*) with MBP−MhpB wild-type as the template, using the external primers shown in Table 1 and the internal primers shown in the table with the codons altered from the wild-type underlined.

Bacterial Growth and Expression. For production of the MBP−MhpB wild-type enzyme and MBP−MhpB mutants, *E. coli* TB1 host cells (New England Bio-Labs) were transformed with MBP−MhpB wild-type or MBP−MhpB mutants. The cells were grown with shaking (200 rpm) in 2 L flasks containing 500 mL of rich medium and 100 μg/mL ampicillin at 37 °C to $A_{660} = 0.6$. IPTG (0.5 mM) was added to induce expression of the cloned gene, and the cells were grown for an additional 3 h and harvested by centrifugation.

Purification of Fusion MhpB Wild-Type and Mutants. Gene products of fusion MhpB wild-type and mutants were isolated on amylose resin columns. The protein was eluted with a column buffer (20 mM Tris-HCl, pH 7.4, 200 mM NaCl, and 1 mM EDTA) and 10 mM maltose. The fractions

Table 1: Overlapping Internal Primers for Site-Directed Mutagenesis (5′ to 3′ Direction)

mutation	primer
forward	GGAATTCATGCACGCTTATCTTCACTGTCTTTCCCACTCGCCGCTGGT
reverse	GCTCTAGAGCTCAGTTCTC
H115Afor	GGTGGACGCCGGGTTCGC
H115Arev	GCGAACCCGGCGTCCACCTGC
H115Qfor	GGTGGACCAAGGGTTCGC
H115Qrev	GCGAACCCTTGGTCCACCTGC
H115Yfor	GGTGGACTACGGGTTCGC
H115Yrev	GCGAACCCGTAGTCCACCTGC
H179Afor	GGGCTTTCCGCTCAGCCG
H179Arev	CGGCTGAGCGGAAAGCCC
H179Qfor	GGGCTTTCCCAACAGCCG
H179Qrev	CGGCTGTTGGGAAAGCCC
H179Yfor	GGGCTTTCCTACCAGCCG
H179Yrev	CGGCTGGTAGGAAAGCCC
D114Afor	GCAGGTGGCCCACGGGTTCGC
D114Arev	GGGCGAACCCGTGGGCCACCTGC
D114Nfor	GCAGGTGAACCACGGGTTCGC
D114Nrev	GCGAACCCGTGGTTCACCTGC
P181Afor	TTTCCCATCAGGCGCCGGTG
P181Arev	CACCGGCGCCTGATGGGAAA
P181Hfor	TGGGCTTTCCCATCAGCATCCG
P181Hrev	CACCGGATGCTGATGGGAAAGCCCA

were collected, and protein concentration was determined by the method of Bradford (*14*). Enzyme purity was analyzed on 11% SDS−PAGE gels, according to standard procedures (*15*). All steps were carried out at 4 °C, unless indicated otherwise. Purified enzymes were >95% purity as judged by SDS−PAGE. Enzymes were concentrated to 1−4 mg/mL using a Centricon ultrafiltration device and were stored in the above buffer containing 50% glycerol at −80 °C.

Circular Dichroism (CD) Spectroscopy. CD spectra were measured over the range of 185−260 nm using a Jasco spectropolarimeter model J-175. Measurements were made using 1 cm cell length and protein concentration of 1 mg/mL at 20 °C with 1 s response time and scan rate of 100 nm/min. Spectra were measured eight times and averaged.

Enzyme Assays. MBP−MhpB wild-type and mutants were reactivated by incubation prior to use by addition of 100 mM sodium ascorbate (5 μL) and 100 mM ammonium iron(II) sulfate (5 μL) to 100 μL of purified enzyme on ice for 1 min. The reactivated enzyme was added to a solution of substrate (10 mM) in 50 mM potassium phosphate, pH 8.0 (*3*). Appearance of ring-fission product of 2,3-dihydroxyphenyl propionic acid was observed at 394 nm (ϵ = 15 600 M^{-1} cm^{-1}). K_m determinations were carried out in duplicate, and K_m values were determined by use of Lineweaver−Burk plots. K_{cat} was calculated from the maximum specific activity of reactivated purified enzyme on the basis of catalytic efficiency per 80 kDa subunit.

Determination of pH/Rate Profiles. pH/rate profiles were determined over the range of 5.0−9.0 using the following buffers at 50 mM concentration: pH 5.0−6.0, sodium citrate; pH 5.8−8.4, potassium phosphate; pH 8.4−9.0, glycine−NaOH. The buffers for the pH profile were checked for inhibitory or activating effects on the reaction. MBP−MhpB wild-type and mutants were assayed by addition of reactivated enzyme (see above) to a solution of substrate (10 mM) in 50 mM buffers at different pH and measurement of rate at 394 nm (due to the RFP dienolate form). Measurement at pH < 7.0 was also carried out at 317 nm (due to the RFP dienol form) for the wild-type enzyme, giving a similar profile.

Analysis of Lactone Hydrolysis Half-Reaction. The enzyme-catalyzed hydrolysis of a seven-membered lactone analogue was carried out as described by Sanvoisin et al. (*6*), using HPLC analysis on an Aminex HPX-87H organic acids column 300 mm × 7.8 mm (Bio-Rad) at 0.3 mL/min in 0.005 M sulfuric acid. The reactivated enzyme was added to a solution of 50 mM potassium phosphate, pH 8.0 (1 mL), containing 100 μL of lactone (1 mg mL^{-1}) to give a final concentration of 50 μg. A series of incubations were stopped at different times (0, 1, 5, 10, and 20 min) by addition of 1 M HCl (50 μL). The final volume (1.1 mL) was filtered on Ultrafree-MC (Millipore Corporation, Bedford, MA) and was analyzed by organic acids HPLC. The retention time of the diacid product was 18.0 min.

RESULTS

Analysis of Class III Extradiol Dioxygenase Active Sites. The precise role of active site residues other than the iron(II) ligands in the catalytic mechanism of the extradiol catechol dioxygenases is largely unknown. In the class III extradiol dioxygenase family, it is known from the LigAB X-ray crystal structure (*5*) that His-12, His-61, and Glu-242 (found in MhpB as His-10, His-51, and Glu-270) are the ligands that bind the iron(II) cofactor. Studies of a biomimetic model reaction for extradiol catechol cleavage (*9*) indicate a requirement for a base, to generate the catecholate monoanion, and a requirement for an acidic group, presumably to catalyze the Criegee rearrangement.

Analysis of the active sites of class II and class III extradiol catechol dioxygenases reveals that there are additional acid−base residues in proximity to the iron(II) center, as shown in Figure 2A. In the active site of class II dioxygenase 2,3-dihydroxybiphenyl 1,2-dioxygenase (BphC), His-195 is positioned 4.0 Å from the iron(II) center: this residue has been proposed to act as a base in the catalytic mechanism (*16*). It has been found that replacement of this histidine residue in *Brevibacterium* 3,4-dihydroxyphenylacetate 2,3-dioxygenase by phenylalanine gives intradiol cleavage activity using 2,3-dihydroxybenzoic acid as substrate (*17*). Additional acid−base residues Tyr-250 and His-241 are positioned 3.8 and 4.8 Å, respectively, from the iron(II) center in BphD.

In the active site of class III dioxygenase protocatechuate 4,5-dioxygenase from *Sphingomonas*, there are two additional histidine residues, His-195 and His-127, positioned 4.5 and 3.9 Å, respectively, from the iron(II) center (Figure 2A). Sequence alignment of class III extradiol dioxygenases (see Figure 2B) reveals that His-195 is completely conserved (found as His-179 in *E. coli* MhpB). His-127 is conserved in all but two sequences, 2-aminophenol 1,6-dioxygenase (AmnB) and 3-hydroxyanthranilate dioxygenase (HAO), both of which cleave 2-aminophenol substrates, in which His-127 (found as His-115 in *E. coli* MhpB) is replaced by tyrosine.

Furthermore, Asp-114 immediately preceding His-115 is also highly conserved. In the LigB crystal structure, the carboxylate side chain of Asp-126 is positioned 4−5 Å from the imidazole side chain of His-127 (see Figure 3), suggesting that this aspartate residue might modulate the pK_a of the neighboring histidine residue. Inspection of the LigB structure also revealed that His-195 (His-179 in MhpB) is in a rather hydrophobic environment, positioned close to Leu-197 (Pro-181 in MhpB), which also appears to form a hydrophobic contact with the catechol substrate (see Figure 3). Inspection of amino acid sequence alignments indicates that Leu-197 is found either as leucine or proline (Pro-181 in MhpB), except in AmnB and HAO, where histidine or arginine, respectively, are found in this position.

Expression and Purification of MBP−MhpB Wild-Type and Mutants. The *mhpB* gene was inserted downstream from the *malE* gene of *E. coli*, which encodes maltose-binding protein (MBP), resulting in the expression of an N-terminal MBP fusion protein. Restriction sites *Eco*RI and *Xba*I were selected as the restriction enzymes for the MBP−MhpB wild-type. Ten site-directed mutants were generated by the method of splicing by overlap extension (*13*) with MBP−MhpB wild-type as the template, using external primers, as described in Materials and Methods. His-115 and His-179 were replaced by alanine, glutamine, and tyrosine (as found in AmnB/HAO); Asp-114 was replaced by asparagine and alanine; Pro-181 was replaced by alanine and histidine (as

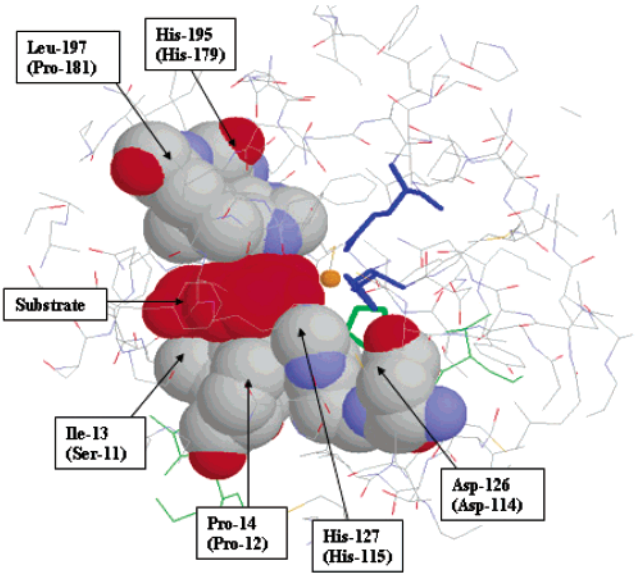

FIGURE 3: Active site environments of His-195 and His-127 in the structure of *Sphingomonas paucimobilis* LigAB. Selected residues and bound substrate are shown in spacefill representation. Iron(II) ligands are shown in wireframe. The picture was prepared using Rasmol. Numbering of selected residues in *E. coli* MhpB sequence is shown in brackets.

Table 2: Kinetic Parameters of MhpB Wild-Type, Fusion MhpB Wild-Type, and Mutant Enzymes

	sp. activity (units/mg)[a]	k_{cat} (s^{-1})[b]	K_m (mM)	k_{cat}/K_m (M^{-1} s^{-1})	lactone hydrolysis?
E. coli MhpB	48	29	0.026	1.1×10^6	yes
MBP−MhpB	40	50	0.050	1.0×10^6	yes
H115Q					no
H115A					yes
H115Y					NT
H179Q					yes
H179A					weak
H179Y					NT
D114N	0.060	0.08	226	0.354	weak
D114A					no
P181A	27.6	11.0	2.74	4.1×10^3	NT
P181H	1.0	0.47	37.8	12.0	NT

[a] Specific activity for MBP−MhpB wild-type and mutants was determined using 10 mM DHP in 50 mM potassium phosphate, pH 8.0, assayed as described in Materials and Methods. [b] k_{cat} was calculated using a molecular weight of 80 kDa for MBP−MhpB wild-type. NT = not tested.

found in AmnB). The MBP−MhpB wild-type and mutants were overexpressed as maltose binding protein fusions in *E. coli* TB1, allowing rapid purification of mutant enzymes using amylose chromatography to >95% purity and high yield. It was found that the MBP−MhpB fusion protein had similar specific activity (40 U/mg) to the native MhpB enzyme (48 U/mg) with a 2-fold higher k_{cat} but 2-fold higher K_m value, as shown in Table 2. Therefore, the activity of mutant enzymes was determined as their MBP fusions. Analysis by circular dichroism spectroscopy of each mutant enzyme gave identical spectra (data not shown), indicating that site-directed mutagenesis of individual residues did not significantly affect protein secondary structure.

Kinetic Characterization of Site-Directed Mutants. The purified MBP−MhpB and the mutants (H115A, H115Q, H115Y, H1179A, H179Q, H179Y, D114A, D114N, P181A, and P181H) were assayed for catalytic activity. Extradiol cleavage can be conveniently assayed by UV/vis spectroscopy, since the extradiol cleavage products absorb at 380−400 nm at pH 8.0. The six mutants at His-179 and His-115 (H115A, H115Q, H115Y, H179A, H179Q, and H179Y) each showed no activity for extradiol cleavage. Although small changes in A_{394} were detected (<0.002 A/min), similar changes were observed in control assays containing no enzyme, and no λ_{max} was observed at 394 nm; thus, we conclude that these small changes are due to the formation of iron−catechol complexes (λ_{max} = 450−500 nm). Therefore, within the detection limits of the assay, replacement of His-115 or His-179 leads to complete loss of extradiol cleavage activity (see Table 2).

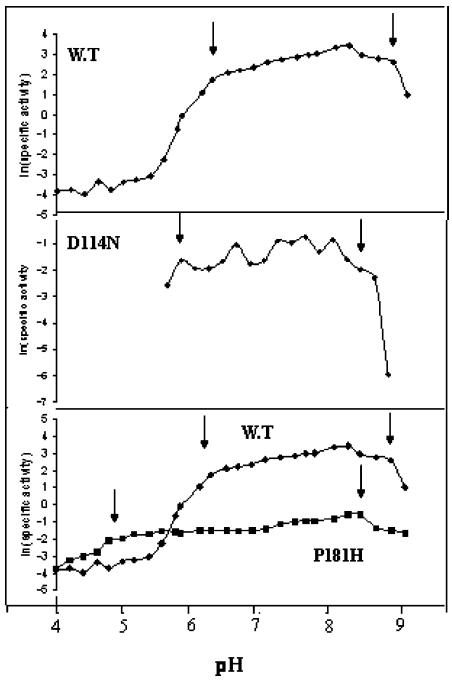

FIGURE 4: pH/rate profiles for wild-type and mutant MBP−MhpB enzymes over pH 5.0−9.0, obtained as described in Materials and Methods: (A) wild-type MBP−MhpB; (B) D114N MBP−MhpB; (C) P181H MBP−MhpB (■), compared with wild-type enzyme (◆).

For the mutations at Asp-114, no catalytic activity could be detected for the D114A mutant, but mutant D114N retained a low level of catalytic activity (0.06 U/mg), 600-fold lower than the wild-type enzyme (see Table 2). The hydrophobic residue adjacent to His-179 (Leu-197 in LigB structure (5)), found as Pro-181 in MhpB, was changed to alanine and histidine. Mutant P181A had a specific activity of 28 U/mg, similar to the wild-type enzyme, but with a 100-fold higher K_m value of 2.7 mM. Mutant P181H had a much lower specific activity of 1 U/mg and a 2-fold reduced k_{cat} (see Table 2).

pH Dependence of MBP−MhpB Wild-Type and Mutant Enzymes D114N, P181A, and P181H. To examine the effect of mutations upon acid/base catalysis, the pH/rate profile for V_{max} was determined for the MBP−MhpB wild-type and mutant enzymes D114N, P181A, and P181H over the pH range from 5 to 9.0 at 50 mM buffer concentration. Measurements at pH > 9.0 were found to be unreliable, due to an additional base-catalyzed nonenzymatic reaction involving iron(II) and catechol substrates.

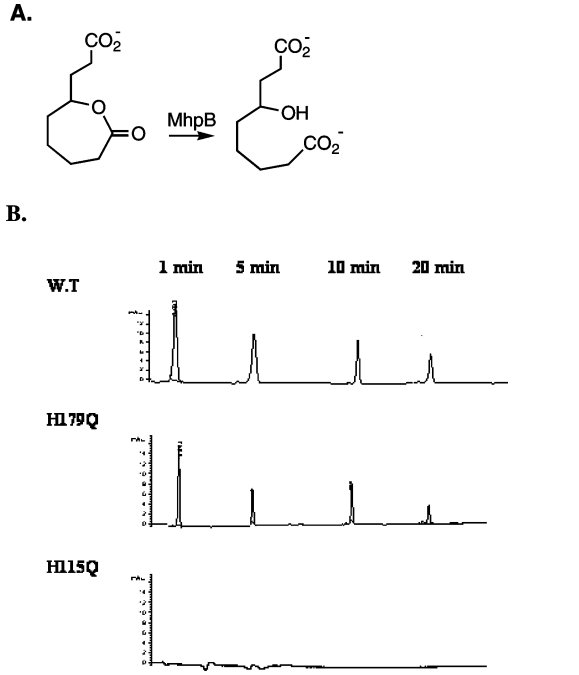

FIGURE 5: Hydrolysis of seven-membered lactone analogue. The reaction is illustrated in panel A. Panel B presents HPLC chromatograms showing diacid product formed vs incubation time for wild-type MBP−MhpB and H179Q mutant but not by H115Q mutant.

As shown in Figure 4, MBP−wild-type MhpB displays a rather complex pH profile, which can be compared with those of the mutant enzymes. Wild-type enzyme shows a small inflection at pH 6.4 and a large inflection at pH 8.8, indicating a catalytic base of pK_a 6.4 and a proton donor of pK_a 8.8. Mutant D114N showed a loss of activity above pH 8.0 with a shift in the higher pK_a to pH 8.0, indicating an effect upon acid catalysis. Mutant P181A and more especially mutant P181H retain more activity than wild-type enzyme at pH 5.0−6.0 (see Figure 4). The lower pK_a value is shifted from 6.4 to 6.0 in P181A (data not shown) and to 4.8 in the P181H mutant, indicating an effect upon base catalysis.

Analysis of Lactone Hydrolysis Half-Reaction. The final step of the extradiol dioxygenase mechanism is the hydrolysis of a seven-membered α-keto lactone intermediate. MhpB has previously been shown to catalyze the hydrolysis of a saturated seven-membered lactone analogue (*6*). The site-directed mutants H115A, H115Q, H115Y, H179A, H179Q, H179Y, D114A, and D114N were therefore analyzed for their ability to catalyze the hydrolysis of this seven-membered lactone analogue, monitoring the hydrolysis by HPLC. Incubation of reactivated enzyme with 0.1 mg/mL lactone at pH 8.0 was monitored by withdrawal of aliquots after 0, 1, 5, 10, and 20 min, followed by injection onto an organic acids column. For wild-type enzyme, a new peak due to diacid product appeared after 1 min, and its intensity gradually decreased to 20 min (Figure 5). This nonlinear time course was observed previously (*6*) and is thought to be due to the nonlinear kinetics of MhpB and the relactonization of the diacid product. As a result, this assay for lactone hydrolysis is largely qualitative.

Mutant H179Q showed the same activity as wild-type enzyme, even though the H179Q mutant is catalytically inactive for extradiol cleavage, indicating that His-179 is not required for lactone hydrolysis. Mutant H179A showed reduced activity for lactone hydrolysis (26% peak height). Mutant H115Q showed no activity at all for lactone hydrolysis, indicating that His-115 is required for lactone hydrolysis. Lactone hydrolysis was observed for the H115A mutant, which we interpret as catalysis by solvent water binding in the pocket normally occupied by His-115. Mutant D114A showed no activity for lactone hydrolysis, and D114N showed weak activity, supporting the role of His-115 in lactone hydrolysis.

DISCUSSION

Previous mechanistic studies on the extradiol catechol dioxygenases have identified several steps and intermediates in the catalytic mechanism (*18*). The iron(II) cofactor is known both to ligate catecholic hydroxyl groups and to activate dioxygen (*19*). There is evidence from the processing of cyclopropyl-containing substrate analogues for a substrate radical intermediate (*20*), followed by the formation of a proximal hydroperoxide intermediate (*7*), which undergoes a Criegee rearrangement via alkenyl migration to give an unsaturated α-keto lactone (*6*). However, the factors that might influence the processing of the proximal hydroperoxide intermediate to give either extradiol product via alkenyl migration or intradiol product via acyl migration are unknown (*18*). Studies of a biomimetic iron(II)/TACN model reaction for extradiol cleavage have indicated that acid catalysis is required for extradiol selectivity (*9*). The observation that replacement of His-200 in *Brevibacterium fuscum* 3,4-dihydroxyphenylacetate 2,3-dioxygenase by phenylalanine gave a mutant enzyme possessing intradiol cleavage activity highlighted the significance of active site histidine residues in extradiol vs intradiol selectivity (*17*). The results described in this paper give new insight into the roles of two active site histidine residues in the class III extradiol dioxygenases.

Replacement of either His-115 or His-179 in *E. coli* MhpB gives mutant enzymes that lack extradiol cleavage activity, indicating that each of these conserved histidine residues is essential for extradiol dioxygenase catalysis. It seemed likely that these residues were involved in acid/base catalysis and that one or the other histidine corresponded to the catalytic base evident at pK_a 6.4 in the wild-type enzyme pH/rate profile. Therefore, the effect of replacing a nearby residue on the pH/rate behavior of the enzyme was examined. Replacement of Asp-114 (located close in space to His-115) by asparagine gave a weakly active enzyme with diminished activity at pH 8.0−9.0, indicating that this mutation had affected acid catalysis during the reaction mechanism. Conversely, replacement of Pro-181 (close in space to His-179) by alanine or histidine gave mutant enzymes that retained greater catalytic activity at pH 5.0−6.0 than the wild-type enzyme, indicating that these mutations had affected base catalysis during the reaction mechanism. There is evidence both from study of the biomimetic model reaction (*9*) and from study of substrate binding to BphC (*21*) that a single active site base is required in extradiol dioxygenases to generate the catecholate monoanion. Our results imply that His-179 is the active site base in MhpB. Examination of the active site of class III dioxygenase LigB reveals that the related His-195 is positioned close to a catechol hydroxyl group and that the only available space accessible to the iron-

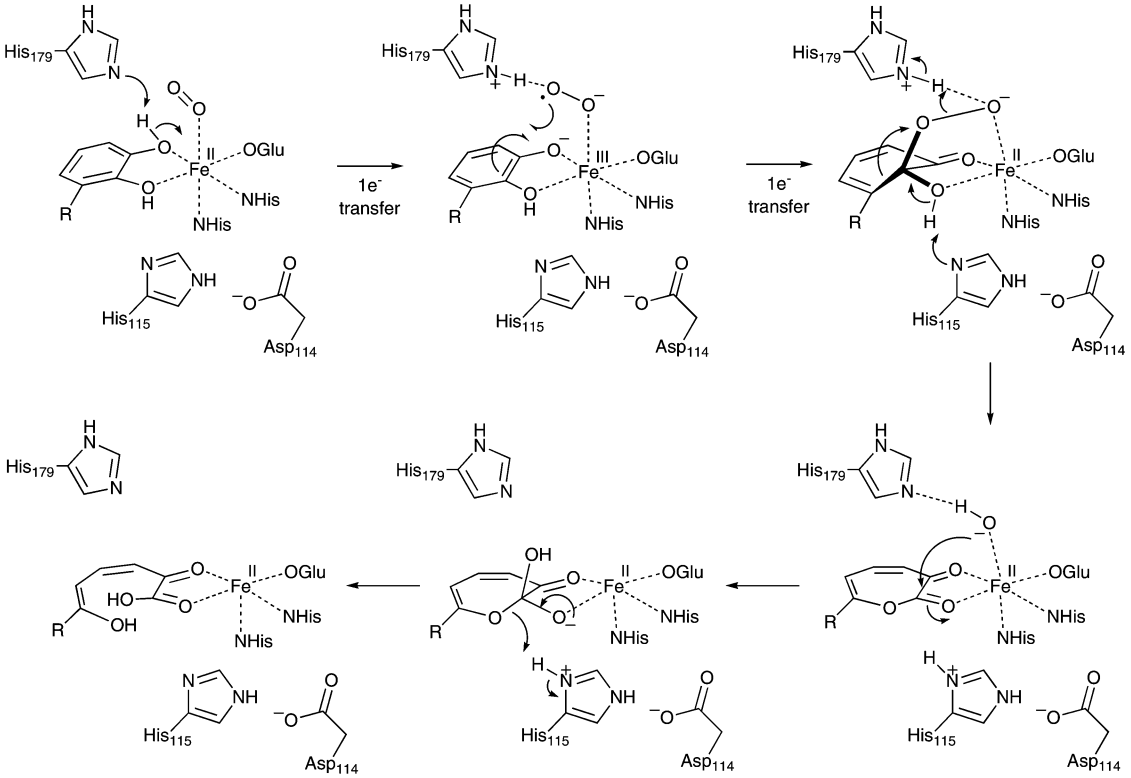

FIGURE 6: Proposed reaction mechanism for extradiol cleavage in MhpB, showing roles of His-179 and His-115 in catalysis. R = $CH_2CH_2CO_2^-$.

(II) cofactor is immediately adjacent to His-195. Therefore, it is very likely that dioxygen is bound close to this residue; consequently the protonated imidazolium side chain of this histidine residue would be able to stabilize the formation of superoxide through one-electron transfer from iron(II) and hence assist oxygen activation. A role for His-195 in class II extradiol dioxygenase BphC in substrate deprotonation and oxygen activation has been suggested by Sato et al. (*16*) on the basis of the structure of the substrate/NO complex. A role for superoxide in oxygen activation is also supported by recent computational studies (*22*).

After deprotonation of the substrate and oxygen activation, the protonated His-179 would be suitably positioned to act as a proton donor to assist in the Creigee rearrangement of the proximal hydroperoxide intermediate. Studies of the iron(II)/TACN extradiol model reaction have shown that acid catalysis is required for extradiol selectivity (*9*), and computational studies have shown that protonation of the proximal oxygen atom bonded to iron(II) provides a low-energy pathway for extradiol cleavage (*22*). Since His-179 would be located immediately adjacent to this proximal oxygen, it seems very likely that it fulfills this role. Subsequently, His-179 appears not to be involved in lactone hydrolysis, since the H179Q mutant has full activity for hydrolysis of the lactone analogue.

His-115 is also shown by these studies to be an essential residue for extradiol dioxygenase catalysis, since the H115Q and H115A mutants are catalytically inactive. The nearby Asp-114 appears to influence the pK_a of His-115, since the D114N mutant is 600-fold less active than the wild-type enzyme and has lost catalytic activity at pH 8.0−9.0. Formation of a histidine−aspartatic acid ion pair would stabilize the imidazolium cation of His-115 and hence increase the pK_a of His-115, making it a stronger base or a weaker acid, yet the loss of activity at higher pH implies an effect upon acid catalysis. The observation that the H115Q mutant is inactive for lactone hydrolysis (unlike the H179Q mutant) implies that His-115 is essential for the final lactone hydrolysis step, probably as an acid catalyst to protonate the hydroxyl leaving group. It seems likely that His-115 is also involved in the Criegee rearrangement step, since no intermediates were detected by single turnover stopped flow analysis in the H115Q mutant (data not shown). Therefore we propose that the Criegee rearrangement involves concerted acid catalysis by His-179 (see above) and deprotonation of the C-3 hydroxyl group by His-115. The protonated His-115 would then subsequently act as an acid catalyst for lactone hydrolysis, as shown in Figure 6. Replacement by tyrosine in AmnB or HAO would in principle allow for acid catalysis by a tyrosine residue, although other residues are presumably involved, since the H115Y mutant was inactive for extradiol cleavage of catechol and 2-aminophenol substrates (data not shown).

These studies have shown that acid−base catalysis is essential for extradiol dioxygenase catalysis and that two suitably positioned histidine residues are utilized for acid−base catalysis in the active sites of the class III extradiol dioxygenases. Each histidine residue appears to have more than one role to play during the catalytic cycle, and the pK_a of each histidine residue appears to be controlled by its microenvironment in the active site. This subtle acid−base catalysis appears to be required only for extradiol cleavage, since the active sites of intradiol catechol dioxygenases do not contain additional acid−base residues; therefore, this appears to be an important distinguishing factor between extradiol and intradiol dioxygenase catalysis.

ACKNOWLEDGMENT

We would like to thank Dr. Gang Lin and Lucy Dalton (University of Warwick) for preliminary work.

REFERENCES

1. Que, L., Jr., and Ho, R. Y. N. (1996) Dioxygen activation by enzymes with mononuclear non-heme iron active sites, *Chem. Rev. 96*, 2607−2624.
2. Bugg, T. D. H. (2003) Dioxygenase enzymes: catalytic mechanisms and chemical models, *Tetrahedron 59*, 7075−7101.
3. Spence, E. L., Kawamukai, M., Sanvoisin, J., Braven, H., and Bugg, T. D. H. (1996) Catechol dioxygenases from *Escherichia coli* (MhpB) and *Alcaligenes eutrophus* (MpcI): sequence analysis and biochemical properties of a third family of extradiol dioxygenases, *J. Bacteriol. 178*, 5449−5256.
4. Han, S., Eltis, L. D., Timmis, K. N., Muchmore, S. W., and Bolin, J. T. (1995) Crystal structure of the biphenyl-cleaving extradiol dioxygenase from a PCB-degrading pseudomonad, *Science 270*, 976−980.
5. Sugimoto, K., Senda, T., Aoshima, H., Masai, E., Fukuda, M., and Mitsui, Y. (1999) Crystal structure of an aromatic ring opening dioxygenase LigAB, a protocatechuate 4,5-dioxygenase, under aerobic conditions, *Structure 7*, 953−965.
6. Sanvoisin, J., Langley, G. J., and Bugg, T. D. H. (1995) Mechanism of the extradiol catechol dioxygenases: evidence for a lactone intermediate in the 2,3-dihydroxyphenylpropionate 1,2-dioxygenase reaction, *J. Am. Chem. Soc. 117*, 7836−7837.
7. Winfield, C. J., Al-Mahrizy, Z., Gravestock, M., and Bugg, T. D. H. (2000) Elucidation of the catalytic mechanisms of the nonhaem iron-dependent catechol dioxygenases: synthesis of carba-analogues for hydroperoxide reaction intermediates, *J. Chem. Soc., Perkin Trans. 1*, 3277−3289.
8. Lin, G., Reid, G., and Bugg, T. D. H. (2000) A biomimetic model reaction for the extradiol catechol dioxygenases, *Chem. Commun.* 1119−1120.
9. Lin, G., Reid, G., and Bugg, T. D. H. (2001) Extradiol oxidative cleavage of catechols by ferrous and ferric complexes of 1,4,7-triazacyclononane: insight into the mechanism of the extradiol catechol dioxygenases, *J. Am. Chem. Soc. 123*, 5030−5039.
10. Davis, J. K., He, Z., Somerville, C. C., and Spain, J. C. (1999) Genetic and biochemical comparison of 2-aminophenol 1,6-dioxygenase of *Pseudomonas pseudoalcaligenes* JS45 to *meta*-cleavage dioxygenases: divergent evolution of 2-aminophenol *meta*-cleavage pathway, *Arch. Microbiol. 172*, 330−339.
11. Malherbe, P., Köhler, C., da Prada, M., Lang, G., Kiefer, V., Schwarcz, R., Lahm, H. W., and Cesura, A. M. (1994) Molecular cloning and functional expression of human 3-hydroxyanthranilic acid dioxygenase, *J. Biol. Chem. 269*, 13792−13797.
12. Blakley, E. R., and Simpson, F. J. (1963) The microbial metabolism of cinnamic acid, *Can. J. Microbiol. 10*, 175−185.
13. Ho, S. N., Hunt, H. D., Horton, R. M., Pullen, J. K., and Pease, L. R. (1989) Site-directed mutagenesis by overlap extension using the polymerase chain reaction, *Gene 77*, 51−59.
14. Bradford, M. M. (1976) A rapid and sensitive method for the quantitation of microgram quantities of protein utilizing the principle of protein dye-binding, *Anal. Biochem. 72*, 248−254.
15. Maniatis, T., Fritsch, E. F., and Sambrook, J. (1982) *Molecular cloning − a laboratory manual*, Cold Spring Harbor Laboratory Press, Cold Spring Harbor, NY.
16. Sato, N., Uragami, Y., Nishizaki, T., Takahashi, Y., Sazaki, G., Sugimoto, K., Nonaka, T., Masai, E., Fukuda, M., and Senda, T. (2002) Crystal structures of the reaction intermediate and its homologue of an extradiol-cleaving dioxygenase, *J. Mol. Biol. 321*, 621−636.
17. Groce, S. L., and Lipscomb, J. D. (2003) Conversion of extradiol aromatic ring-cleaving homoprotocatechuate 2,3-dioxygenase into an intradiol cleaving enzyme, *J. Am. Chem. Soc. 125*, 11780−11781.
18. Bugg, T. D. H., and Lin, G. (2001) Solving the riddle of the intradiol and extradiol catechol dioxygenases: how do enzymes control hydroperoxide rearrangements? *Chem. Commun*. 941−952.
19. Arciero, D. M., and Lipscomb, J. D. (1986) Binding of ^{17}O-labeled substrate and inhibitors to protocatechuate 4,5-dioxygenase-nitrosyl complex: evidence for direct substrate binding to the active site Fe^{2+} of extradiol dioxygenases, *J. Biol. Chem. 261*, 2170−2178.
20. Spence, E. L., Langley, G. J., and Bugg, T. D. H. (1996) Cis−trans isomerization of a cyclopropyl radical trap catalyzed by extradiol catechol dioxygenases: evidence for a semiquinone intermediate, *J. Am. Chem. Soc. 118*, 8336−8343.
21. Vaillancourt, F. H., Barbosa, C. J., Spiro, T. G., Bolin, J. T., Blades, M. W., Turner, R. F. B., and Eltis, L. D. (2002) Definitive evidence for monoanionic binding of 2,3-dihydroxybiphenyl to 2,3-dihydroxybiphenyl 1,2-dioxygenase from UV resonance Raman spectroscopy, UV/vis absorption spectroscopy, and crystallography, *J. Am. Chem. Soc. 124*, 2485−2496.
22. Deeth, R. J., and Bugg, T. D. H. (2003) A density functional investigation of the extradiol cleavage mechanism in non-heme iron catechol dioxygenases, *J. Biol. Inorg. Chem. 8*, 409−418.
23. Barnes, M. R., Duetz, W. A., and Williams, P. A. (1997) A 3-(3-hydroxyphenyl)propionic acid catabolic pathway in *Rhodococcus globerulus* PWD1: cloning and characterization of the *hpp* operon, *J. Bacteriol. 179*, 6145−6153.
24. Arai, H., Yamamoto, T., Ohishi, T., Shimizu, T., Nakata, T., and Kudo, T. (1999) Genetic organization and characteristics of the 3-(3-hydroxyphenyl)propionic acid degradation pathway of *Comamonas testosteroni* TA441. *Microbiology 145*, 2813−2820.
25. Laurie, A. D., and Lloyd-Jones, G. (1999) The *phn* genes of *Burkholderia* sp. strain RP007 constitute a divergent gene cluster for polycyclic aromatic hydrocarbon catabolism, *J. Bacteriol. 181*, 531−540.

BI048518T